SOLID STATE SYNTHESIS OF THE PSEUDO-BINARY OXIDES DOPED WITH V_2O_5 MATERIALS

Mihaela Birdeanu[1, 2], Mirela Vaida[1], Aurel - Valentin Bîrdeanu[3], Francisc Peter[1], Eugenia Fagadar-Cosma[4]

[1] Politehnica University of Timisoara, Vasile Parvan Ave.6, 300223-Timisoara, Romania, e-mail: mihaelabirdeanu@gnail.com, vaida.mirela@yahoo.com francisc.peter@upt.ro
[2] National Institute for Research and Development in Electrochemistry and Condensed Matter, 1 Plautius Andronescu Street, 300224 Timisoara, Romania.
[3] National R&D Institute for Welding and Material Testing - ISIM Timişoara, 20 M. Viteazu Ave., 300222, Timisoara, Romania, e-mail: valentin@isim.ro
[4] Institute of Chemistry Timisoara of Romanian Academy, 24 M. Viteazu Ave, 300223-Timisoara, Romania, e-mail: efagadar@yahoo.com
Corresponding author: vaida.mirela@yahoo.com

ABSTRACT: This paper is focused on the obtaining of materials based on $ZnTa_2O_6$ and $ZnNb_2O_6$ both doped with V_2O_5, by solid state method. To characterize the obtained materials XRD, SEM/EDAX, AFM and UV-Vis analysis were performed. The morphology of the two materials revealed a rod like shape of the particles with more ordered alignment of particles for the second material. EDAX experiments confirmed the structure and composition of the two compounds. UV-Vis analysis was done and further the band gap for each of the materials was determined, having the following values: 4.03 eV and 4.06 eV.

KEYWORDS: solid state, XRD, SEM/EDAX, AFM, band gap

1. INTRODUCTION

The pseudo-binary oxides $ZnTa_2O_6$ and $ZnNb_2O_6$ are both known as materials which act excellent as photocatalyst [1] or for possessing excellent microwave dielectric properties [2-5]. Until now, it was reported various obtaining methods as molten salt synthesis [2], solid state method [6], coprecipitation [3], hydrothermal [7] and also sol-gel [8-10] method. It was shown that the advantages of using molten salt synthesis is that it could control the form and size of the particle, because solid-state and sol-gel methods are offering sometimes a too dispersed size of particle and too high temperatures might be used in obtaining.

The vanadium oxide, V_2O_5, is known as a precursor widely used in obtaining materials as: wurtzite, phosphor materials or vanadate glasses, often in combination with ZnO [11-13].

In the present paper, results regarding the obtaining through the solid state synthesis method and characterization of $ZnTa_2O_6$ and of the $ZnNb_2O_6$ materials both doped with V_2O_5 materials are presented.

2. EXPERIMENTAL

1. Solid state synthesis of the $ZnTa_2O_6$ and $ZnNb_2O_6$, both doped with V_2O_5

The materials $ZnTa_2O_6$ and $ZnNb_2O_6$, both doped with V_2O_5, were obtained through the solid state method. The precursors that were used are: the pseudo-binary oxide $ZnTa_2O_6$ obtained at 1100^oC through the solid-state method as it was described in [14], the pseudo-binary oxide $ZnNb_2O_6$ obtained by the same solid-state method and tantalum pentaoxide (V_2O_5) (99, 6 % purity, Sigma).
The obtained mixtures using the molar ratio $(ZnTa_2O_6)0.9$ and $(V_2O_5)0.1$, $(ZnNb_2O_6)0.9$ and $(V_2O_5)0.1$ were syntherized in an calcination oven at 600^0C for 6 h/each sample. The heating and cooling rate of the oven was 5ºC/min.

2. Characterization techniques:

The characterizations have been performed on well crystallized powder samples of materials.
The phase identification of the synthesized powders was performed using X-ray diffraction (XRD) with monochromatic Cu Kα (λ = 1.5418 Å) incident radiation on an X'pert Pro MPD X-ray Diffraction data were obtained for the angular range $2\theta = 10\text{-}80^0$ using a 0.020 step and the counting time was 5 s.
To determinate the morphology and the particle's dimension of the samples, the field emission-scanning electron microscopy – SEM (Model INSPECT S) and Atomic Force microscopy - AFM (Model Nanosurf® EasyScan 2 Advanced Research) were used. The optical band gap of both materials was calculated by recording the diffuse reflectance

spectrum at room temperature, using a UV-VIS-NIR spectrometer Lambda 950.

3. RESULTS AND DISCUSSIONS

1. Quality determination of pseudo-binary oxides materials using XRD

In figures 1 and 2 are presented the X-ray diffraction spectra of the $ZnTa_2O_6$ and $ZnNb_2O_6$ materials doped with V_2O_5 compared with the XRD spectra of the $ZnTa_2O_6$ respectively $ZnNb_2O_6$ materials. Also, in these figures the most intense peaks magnified are inserted and it can be observed that the $ZnTa_2O_6$ doped with V_2O_5, respectively $ZnNb_2O_6$ doped with V_2O_5 spectra are shifted to the left, due to the fact that the ionic radii of the dopant (V) is smaller than the ionic radii of the element that V substitutes (Ta respectively Nb).

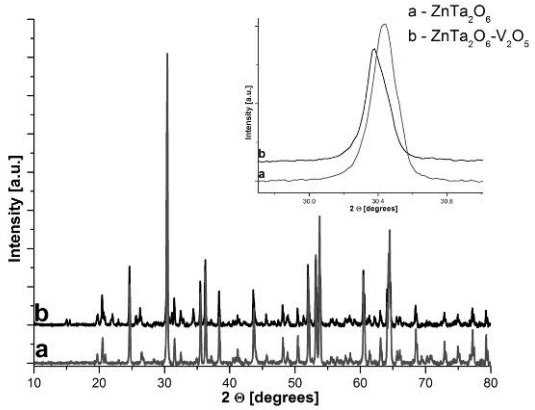

Figure 1. The diffraction spectra of the $ZnTa_2O_6$ doped with V_2O_5 and $ZnTa_2O_6$. In the right upper part of the plot is presented the magnified spectra of the most intense peak.

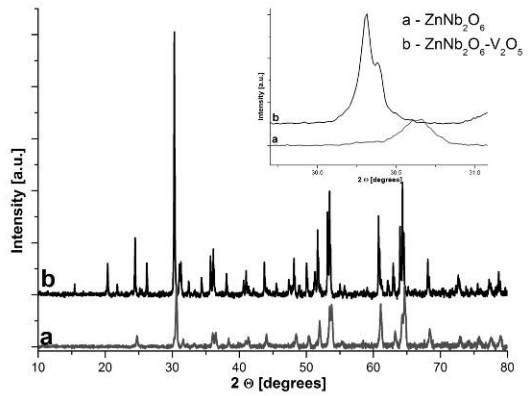

Figure 2. The diffraction spectra of the $ZnNb_2O_6$ doped with V_2O_5 and $ZnNb_2O_6$. In the right upper part of the plot is presented the magnified spectra of the most intense peak.

2. The morphologic and crystallites size study for $ZnTa_2O_6$ doped with V_2O_5 and $ZnNb_2O_6$ doped with V_2O_5

In Figure 3(a), from SEM image, it can be observed that the shape of the particles for $ZnTa_2O_6$ doped with V_2O_5 is rod like. For $ZnNb_2O_6$ doped with V_2O_5 (figure 4(a)), the same rod like shape is noticed which confirms the previously reported experiments [2, 6], with the observation that the image reveal smaller rods in a more ordered form, oriented by a direction reporting to the $ZnTa_2O_6$ doped with V_2O_5.

From the EDAX images, (figures 3(b) and 4(b)), only the Zn, V, Ta and respectively Nb peaks can be observed which demonstrate the material composition.

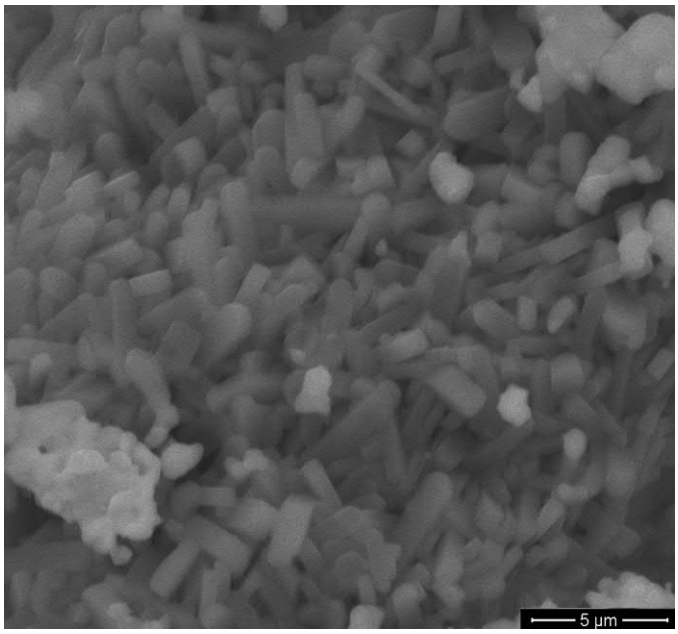

(a)

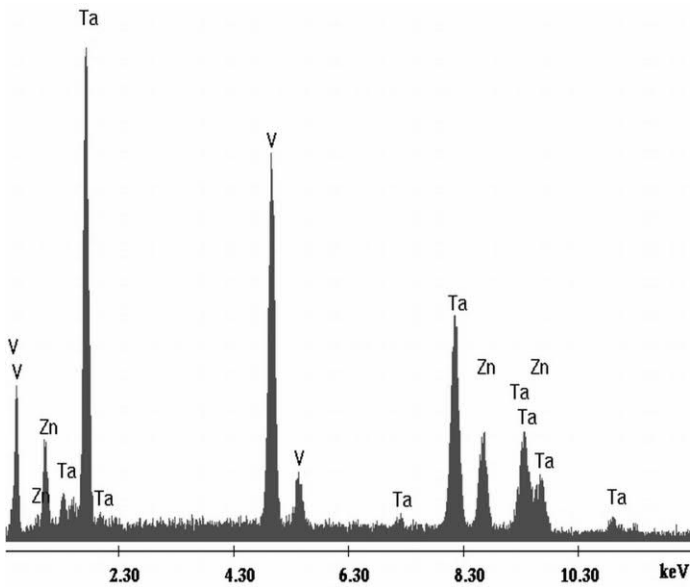

(b)

Figure 3. SEM (a) and EDAX (b) images for $ZnTa_2O_6$ doped with V_2O_5 obtained at 600^0C with a 6 h reaction time

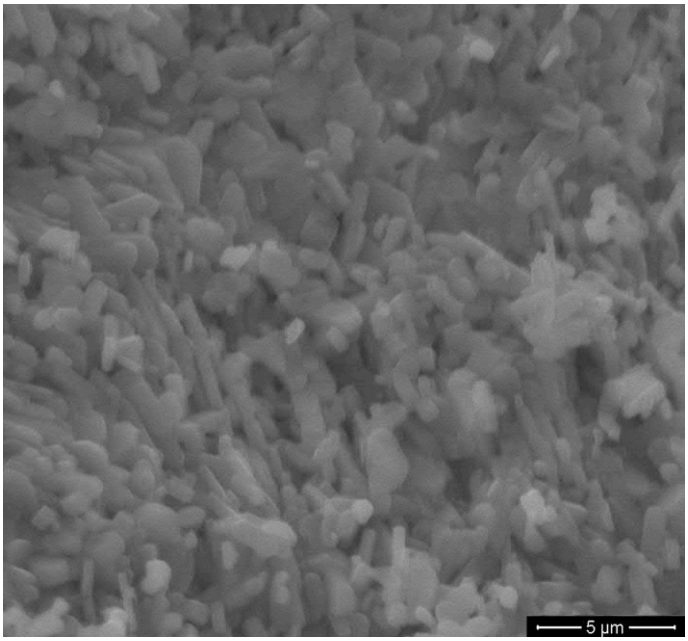

(a)

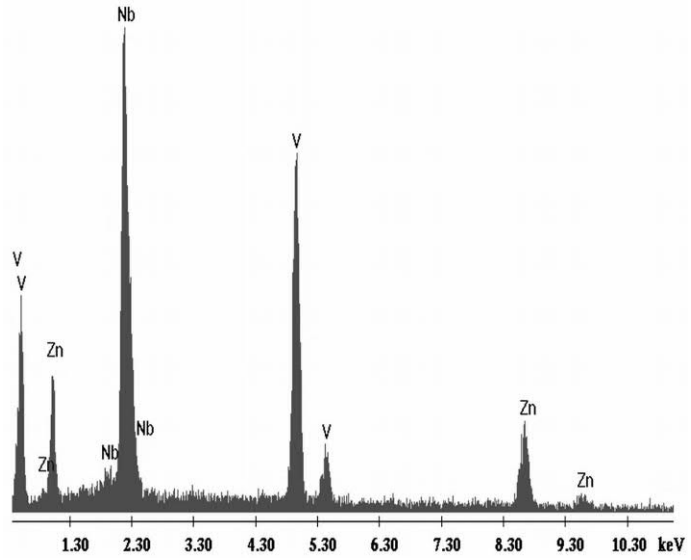

(b)

Figure 4. SEM (a) and EDAX (b) images for $ZnNb_2O_6$ doped with V_2O_5 obtained at 600^0C with a 6 h reaction time

To confirm the results obtained from the SEM measurements, AFM measurements were realised in the contact mode on a surface of about 1µm x 1 µm for each material. From figure 5 (a) it can be observed the topographical map for $ZnTa_2O_6$ doped with V_2O_5 and from figure 5(b) the size of the particles which is between 1 and 2.5 nm. From figure 5 (c) it can be seen that the particles are uniformly arranged on the analysed surface.

The AFM images of $ZnNb_2O_6$ doped with V_2O_5 are presented in figure 6. The 3D topographical map of the material in presented in figure 6 (a). From figure 6(b) it was noticed that the particles size is between 2 and 4 nm. Figure 6 (c) shows an uniformly distribution of the particles on the analysed surface.

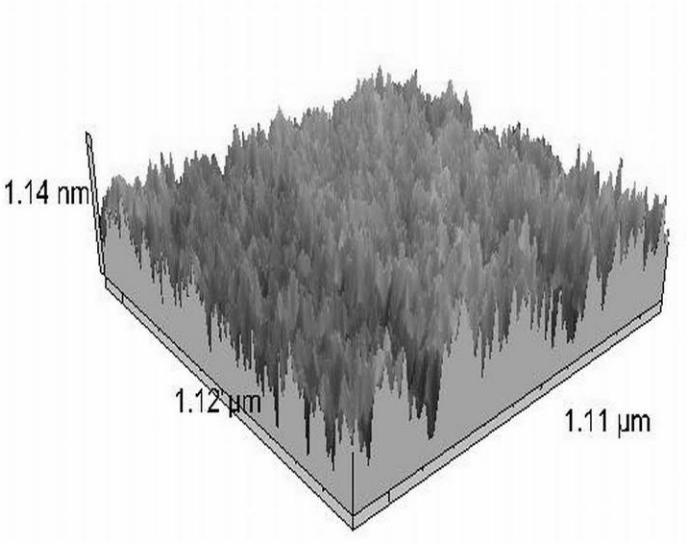

(a)

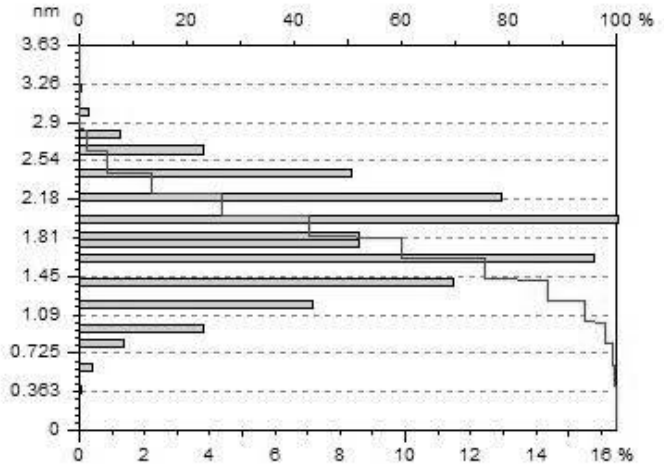

(b)

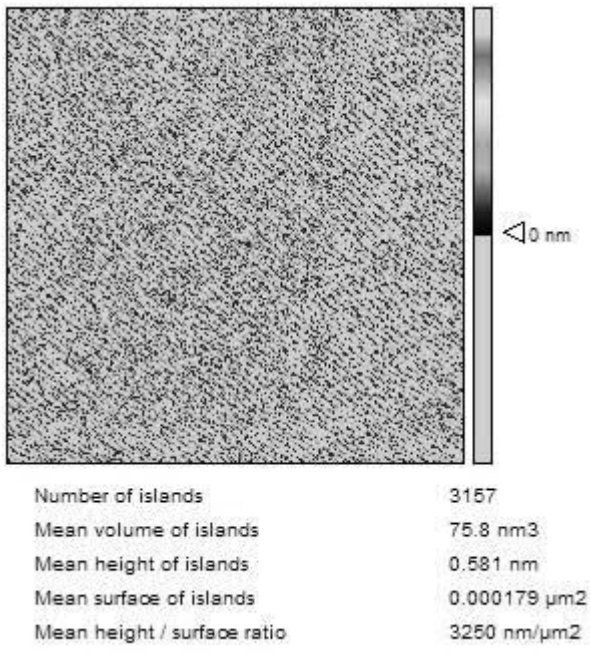

(c)

Figure 5. The AFM images of $ZnTa_2O_6$ doped with V_2O_5 representing: a) the 3D topographical map; b) Height

distributions of the particles; c) The particles distribution on the scanned surfaces

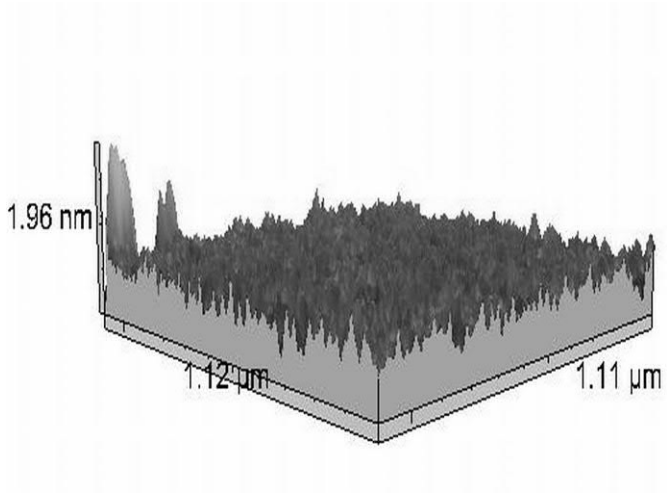

(a)

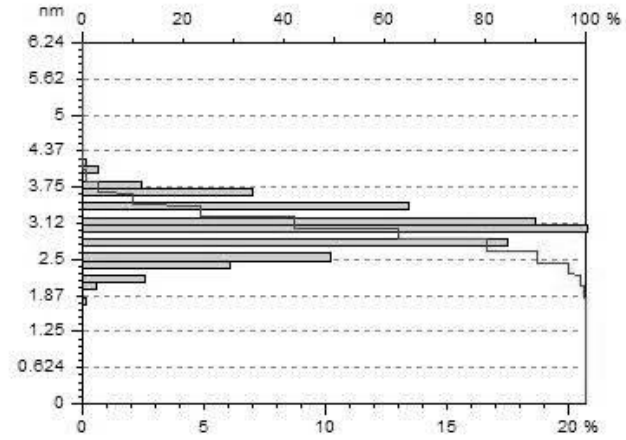

(b)

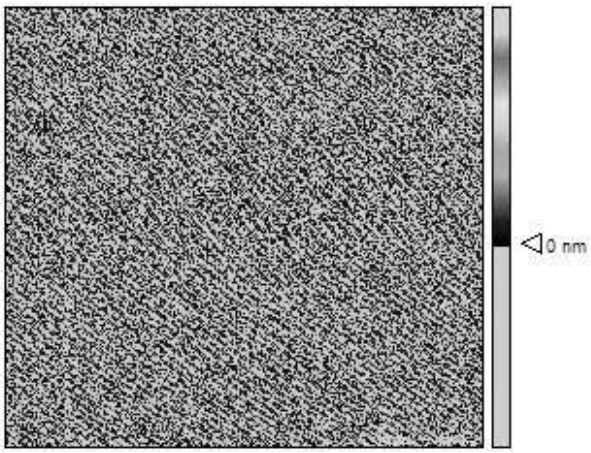

Number of islands	3179
Mean volume of islands	51.5 nm3
Mean height of islands	0.46 nm
Mean surface of islands	0.000199 µm2
Mean height / surface ratio	2316 nm/µm2

(c)

Figure 6. The AFM images of $ZnNb_2O_6$ doped with V_2O_5 representing: a) the 3D topographical map; b) Height distributions of the particles; c) The particles distribution on the scanned surfaces

Using the following equations for the average surface roughness and the root mean squared surface roughness's calculations [15]:

$$S_a = \frac{1}{mn}\sum_{j=1}^{n}\sum_{i=1}^{m}|z_{ij}| \quad (1)$$

$$S_q = \sqrt{\frac{1}{mn}\sum_{i=1}^{m}\sum_{j=1}^{n} z^2\,(x_i, y_i)} \quad (2)$$

S_a and S_q were determined for an area A=1.312 pm^2 (see Table 1). In equations (1) and (2) m and n represent the number of the particles on x and y axis, with z-the medium high of the particles, x_k and y_l represent the minimum and the maximum deviations of the particles related to the medium value.

Table 1. The calculated roughness for the $ZnTa_2O_6$ and $ZnNb_2O_6$ doped with V_2O_5 materials

Material	S_a	S_q
$ZnTa_2O_6$ doped with V_2O_5	0.1 nm	0.18 nm
$ZnNb_2O_6$ doped with V_2O_5	0.096 nm	0.17 nm

3.3. The optical properties of the $ZnTa_2O_6$ and $ZnNb_2O_6$ doped with V_2O_5 materials

Using the Kubelka-Munk equations [16, 17], from the reflectance spectrum, the absorbance was calculated (Figure 7). Using the absorbance spectra, the band gap was determined. $\{(k/s)h\nu\}^2$ versus $h\nu$ plot was inserted in figure 7.

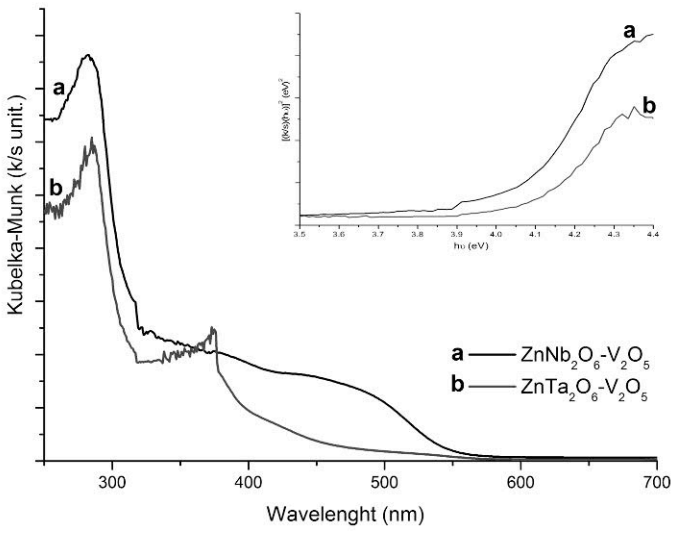

Figure 7. The absorbance spectrum of: $ZnTa_2O_6$ doped with V_2O_5 and $ZnNb_2O_6$ doped with V_2O_5 . vs. hν (energy was inserted for: $ZnTa_2O_6$ doped with V_2O_5 and $ZnNb_2O_6$ doped with V_2O_5

For $ZnTa_2O_6$ doped with V_2O_5, the band gap value was found to be 4.06 eV and respectively, 4.03 eV for $ZnNb_2O_6$ doped with V_2O_5. For this second

material was reported in the literature [10] the same value for the band gap (4.0eV).

4. CONCLUSIONS

This paper is devoted to the obtaining of $ZnTa_2O_6$ and of $ZnNb_2O_6$ both doped with V_2O_5 through the solid state method at 600^{o}C. XRD experiments show that both materials were formed, the most intense peaks being shifted to left, due to the smaller ionic radii of the dopant V ions which substitute the Ta respectively the Nb ions in the pseudo-binary oxides materials: $ZnTa_2O_6$ and $ZnNb_2O_6$. SEM/EDAX images revealed in both cases a rod like shape of the particles, which for the second analysed material are aligned according with a direction. The morphology and the size of particles were confirmed by the AFM measurements. UV-Vis analyses were made and further it was calculated the band gap for each of the materials, for $ZnTa_2O_6$ doped with V_2O_5, the band gap value was found to be 4.06 eV and respectively, 4.03 eV for $ZnNb_2O_6$ doped with V_2O_5.

5. ACKNOWLEDGEMENTS

This paper is partially supported by the Sectoral Operational Programme Human Resources Development (SOP HRD), financed from the European Social Fund and by the Romanian Government under the project number POSDRU/159/1.5/S/134378.
This work was partially supported by the strategic grant POSDRU/159/1.5/S/137070 (2014) of the Ministry of National Education, Romania, co-financed by the European Social Fund – Investing in People, within the Sectoral Operational Programme Human Resources Development 2007-2013.
The author Eugenia Fagadar-Cosma is acknowledging Romanian Academy for financial support in the frame of Programme 3 of ICT-AR.

6. REFERENCES

1. Ding Z., Wu W., Liang S., Zheng H., Wu L., Selective-syntheses, characterizations and photocatalytic activities of nanocrystalline $ZnTa_2O_6$ photocatalysts, *Mat. Lett*., Vol. 65, pp. 1598- 1600, (2011).

2. Guo, L., Dai, J., Tian, J., Zhu, Z., He, T., Molten salt synthesis of $ZnNb_2O_6$ powder, *Mater. Res. Bull.,* Vol. 42, pp. 2013–2016, (2007).

3. Deshpande, V. V., Patil, M. M., Navale, S. C., Ravi, V., A coprecipitation technique to prepare $ZnNb_2O_6$ powders, *Bull. Mater. Sci*., Vol. 28, pp. 205– 207, (2005).

4. Hsiao, Y.-J., Fang, T.-H., Ji, L.-W., Synthesis and luminescent properties of $ZnNb_2O_6$ nanocrystals for solar cell, *Mater. Lett.,* Vol.64, pp. 2563–2565, (2010).

5. Guo, L., Dai, J., Tian, J., He, T., Synthesis of $ZnNb_2O_6$ powder with rod-like particle morphologies, *Ceram. Int*., Vol.34, pp. 1783–1785, (2008).

6. Feng, G., Jiaji, L., Rongzi, H., Zhen, L., Changsheng, T., Microstructure and dielectric properties of low temperature sintered $ZnNb_2O_6$ microwave ceramics, *Ceram. Int*., Vol.35, pp. 2687–2692, (2009).

7. Dai, J., Zhang, C., Shi, L., Song, W., Wu, P., Huang, X., Low-temperature synthesis of $ZnNb_2O_6$ powders via hydrothermal method, *Ceram. Int.,* Vol. 38, pp. 1211–1214, (2012).

8. Hsiao, Y.-J., Fang, T.-H., Ji, L.-W., Synthesis and luminescent properties of $ZnNb_2O_6$ nanocrystals for solar cell, *Mater. Lett*., Vol. 64, pp. 2563 – 2565, (2010).

9. Hsu, C.-H., Yang, P.-C., Yang, H.-W., Yan, S.-F.,Tung H. H., Study and fabrication of $ZnNb_2O_6$ thin films by sol–gel method, *Thin Sol. Films,* Vol. 519, pp. 5030–5032, (2011).

10. Wu, W., Liang, S., Ding, Z., Zheng, H., Wu, L., Low temperature synthesis of nanosized $ZnNb_2O_6$ photocatalysts by a citrate complex method*, J. Sol-Gel Sci. Technol*., Vol. 61, pp. 570–576, (2012).

11. Li, T., Luo, J., Honda, Z., Fukuda, T., Kamata, N., Sintering Condition and Optical Properties of $Zn_3V_2O_8$ Phosphor, *Adv. Math. Phys. Chem*., Vol. 2, pp. 173-177, (2012).

12. Lopez-Calzada, G., Pancardo-Rodriguez, I., Carmona-Rodriguez, J., Zayas, M. E., Rodriguez- Melgarejo, F., Martinez-Juarez, J., Juarez-Diaz, G., Zelaya-Angel, O., Portillo-Moreno, O., Jimenez- Sandoval, S. J., Lozada-Morales, R., Local order effects on the photoluminescence of Er^{3+} in a novel vitreous matrix of the $CdO-ZnO-V_2O_5$ system and manifolds in $Zn_xAl_{2-x}O_3$ micro crystalline aggregates, *Opt. Mater*,. Vol. 32, pp. 1090- 1094, (2010).

13. Chen, Z., Chen, D., Lv, P., Yan, F., Zhan, Z., Li, B. Huang, F., Liang, J., Subsolidus phase relationships in the system $ZnO–V_2O_5–WO_3$

research on suitable flux for ZnO crystal growth, *J. Alloy. Compd*., Vol. 476, pp. 241-244, (2009).

14. Birdeanu, M., Birdeanu, A.–V., Fagadar- Cosma, E., Enache, C., Miron, I., Grozescu, I., Structural, morphological, optical and thermal properties of the $ZnTa_2O_6$ nanomaterials obtained by solid – state method, *Digest J. Nanomater. Bios*., Vol. 8, pp. 263 – 272, (2013).
15. Johnson, D., Hilal, N., Characterisation and quantification of membrane surface properties using atomic force microscopy: A comprehensive review, *Desalination,* Vol. 356, pp. 149- 164, (2015).
16. Kubelka, P., Munk F. Ein Beitrag zur Optik der Farban-striche. Zh Tekh Fiz., Vol. 12, pp. 593-607, (1931).
17. Kubelka, P., New contribution to the optics of intensely light-scattering materials. Part I, *J. Opt Soc. Am.*, Vol. 38, pp. 448-57, (1948).